



# Probabilistic Seismic Hazard Assessment of Pakistan Territory Using an Areal Source Model

MUHAMMAD WASEEM,<sup>1</sup> SARFRAZ KHAN,<sup>2</sup> and M. ASIF KHAN<sup>2</sup>

**Abstract**—A seismic hazard map for the national seismic design code of Pakistan (i.e., Building Code of Pakistan) is derived using probabilistic seismic hazard assessment (PSHA) approach. In order to update the seismic code, an updated seismic zoning map is required that should be based on usage of the recent seismic hazard elements. PSHA of Pakistan is an essential and important milestone. For this purpose, the standard Cornell–McGuire (1968–1976) approach is employed, and the computations are made over a rectangular grid of  $0.1^\circ$ . The main features of this study include usage of a recently compiled earthquake catalogue, recent ground motion prediction equations and an updated seismic source model. The resulting ground motions are obtained as peak ground acceleration (PGA) and 5% damped spectral acceleration (SA) at  $T = 0.2$  s and  $T = 1.0$  s for 475-, 975- and 2475-year return periods (RPs) (evaluated for the flat rock site conditions). Results of the study show that seismic hazard in Pakistan is highest in its central and northern parts. In the central part near Quetta, severe seismic hazard (PGA 0.40 g) is observed. Among the important cities in Pakistan, Balakot city is likely to experience a PGA value of 0.36 g, while Islamabad, Peshawar and Chitral are likely to experience 0.33 g. The cities of Gilgit, Karachi and Gwadar experience ground motion values of 0.34, 0.26 and 0.29 g, respectively, for the 475-year return period (RP). It has also been observed that ground motion values show variation in the distribution and magnitude in contrast to the hazard map of national design code. The hazard map presented in this study is the improved seismic hazard zoning map of Pakistan that would be helpful in developing pre-disaster mitigation strategies and risk assessment studies in Pakistan. It is concluded that the seismic zoning map of the national seismic design code of Pakistan underestimates the ground motion values, and it should be updated or replaced.

**Keywords:** Pakistan, probabilistic seismic hazard assessment, area source model, earthquake catalogue, building code of Pakistan.

---

**Electronic supplementary material** The online version of this article (<https://doi.org/10.1007/s00024-020-02455-7>) contains supplementary material, which is available to authorized users.

---

<sup>1</sup> Department of Civil Engineering, University of Engineering and Technology, Peshawar, Pakistan. E-mail: [eec\\_pesh@yahoo.com](mailto:eec_pesh@yahoo.com)

<sup>2</sup> National Centre of Excellence in Geology, University of Peshawar, Peshawar, Pakistan.

## 1. Introduction

Pakistan is geographically located in one of the most seismically active regions of the world due to its tectonic settings. The tectonic settings of Pakistan are unique, as three major tectonic plates are converging to its location. It is exposed to very high seismic risk because of vulnerability of the built structures due to poor construction practices in the country. Besides these practices, the presence of seismically active features (i.e., Himalayan, HinduKush, Makran, Kirthar and Sulaiman ranges, etc.) in and around Pakistan are potential threats for future earthquakes.

Looking at its seismic hazard assessment efforts, we come across the Building Code of Pakistan (1986) followed by the efforts of the Global Seismic Hazard Assessment Program (e.g., Zhang et al. 1999; Shedlock et al. 2000). Zhang et al. (1999) represents the first ever probabilistic seismic hazard assessment (PSHA) application concerning Pakistan. Later, seismic provisions for the building code were introduced in 2007, which included a PSHA-based seismic zoning map of Pakistan. After 2010, the efforts of Rafi et al. (2012) and Zaman et al. (2012) emerged as country-based studies. Rafi et al. (2012) utilized a classical approach, and Zaman et al. (2012) used the Frankel (1995) approach to produce hazard maps. More recently, the Earthquake Model of Middle East (EMME) project results by Sesetyan et al. (2018b) were published that also include a seismic hazard map of Pakistan.

The PSHA approach is a popular way to estimate seismic hazard. Some of the notable PSHA-based studies around Pakistan and surroundings include Nath and Thingbaijam's (2012) seismic hazard assessment study for India, the seismic hazard assessment performed by Rahman and Bai (2018) for Nepal, the PSHA carried out by Rahman et al. (2017)

for the Himalayan and Tibetan regions, the hazard study by Sawires et al. (2016) for Egypt, and Stevens and Avouac (2015) work on inter-seismic coupling of the Himalayan frontal thrust.

In PSHA, uncertainties in the size and location of earthquakes and in the variation of the ground motion intensity are identified, quantified and combined to describe a complete picture of seismic hazard (Kramer 1996). These variations are modelled with probability density functions (PDFs), and the rate of earthquakes having ground motion values greater than or equal to a threshold magnitude is then determined. The final result of PSHA is obtained as a curve between annual rate and ground motion amplitudes. PSHA was first proposed by Cornell (1968) and later on coded in FORTRAN by McGuire (1976). The Cornell (1968) and McGuire (1976) approach is based on Poissonian probability distribution of earthquakes. The seismicity rate is constant within the sources and does not vary.

Besides the standard approach, kernel estimation methods (i.e., Frankel 1995; Woo 1996) of PSHA are also being practiced due to subjectivity involved in the delineation of source models. Rahman et al. (2017) and Rahman and Bai (2018) have implemented these methods. In this study, a standard approach has been implemented due to (1) the limited span of the earthquake catalogue and (2) faults not being very well characterized in Pakistan.

Earthquake mitigation measures are connected with the reliable estimates of seismic hazard. These mitigation measures include earthquake-resistant design policies, earthquake vulnerability and regional loss estimation models. Since Pakistan is a developing country where urbanization growth is higher, it is therefore imperative to recalculate the seismic hazard in its territory as a step towards the mitigation measures against the expected earthquake damage.

All the previous studies, including the most recent by Sesetyan et al. (2018b), have defined hazard in terms of PGA values. None of these studies has reported the hazard in terms of spectral intensities, and thus seismic hazard maps in terms of the spectral intensity are needed to fill the gap left by these studies. Spectral intensity values are required for the seismic design of bridges in Pakistan using the American Association of State Highway and

Transportation Officials (AASHTO) code and the International Building Code (IBC). The IBC will replace the Uniform Building Code (UBC) in the upcoming version of the building code of Pakistan.

The basic aim of this study is to perform PSHA of Pakistan using a recently updated earthquake catalogue, a new seismic source model and ground motion prediction equations in order to define ground motion in terms of PGA and spectral acceleration (SA) values at 0.2 s and 1.0 s, which is consistent with current code practices in Pakistan.

## 2. General Information on Seismotectonics and the Current Building Code of Pakistan

Pakistan is located in a seismically active region due to the active nature of the tectonic features attributed to the plate boundaries of three major mutually converging tectonic plates (i.e., Arabian, Indian and Eurasian). The Indian plate is located north of Pakistan and moves at a rate of  $20.5 \pm 1$  mm/year near western Nepal (Ader et al. 2012) with respect to the Eurasian plate. In the south of Pakistan, the Arabian and Eurasian plates are interacting with each other. The Arabian plate is subducting underneath the Eurasian plate at a rate of 28–33 mm/year (Apel et al. 2006). Active tectonic features (e.g., HinduKush, Himalayan, Pamir, Sulaiman and Kirthar mountain ranges) are formed due to the interaction of these plates. In the northwest of Pakistan, the HinduKush–Pamir range (the most active potential seismic source contributor in the world) formed at the junction of the Balochistan arc, Himalaya, Pamir and Karakorum Mountains ranges (Desio 1963). An active subduction zone known as the Makran subduction zone is also located in the western south coast of Pakistan formed by interaction of the Arabian and Indian plates. The great earthquake of Makran, which caused a tsunami in the Arabian Sea, took place at the Makran subduction zone (Rafi et al. 2012).

Pakistan has a history of experiencing the deadliest historical regional earthquakes in the last 100 years that have caused damage to the infrastructure and loss of human lives [e.g., 1935 Quetta earthquake ( $M_w = 7.8$ ); 1945 Makran earthquake

( $M_w = 8.2$ ); 2005 Kashmir earthquake ( $M_w = 7.6$ ); 2008 Awaran earthquake ( $M_w = 7.7$ )]. Major earthquakes ( $M > 6.5$ ) in and around Pakistan along with the plate boundaries are shown in Fig. 1 (modified from Khan et al. 2018). The details about these events are comprehensively provided in Khan et al. (2018). These events show that earthquakes with magnitude 7.0 have occurred in this part of the world, and they may occur in this region in the future. These earthquakes show high seismic hazard exists in and around Pakistan. The historical earthquakes also provide information about the maximum magnitude potential

for seismic sources via the Cornell–McGuire approach. The 25 AD Taxila earthquake of magnitude 7.5 represents the earliest recorded earthquake concerning Pakistan. Epicenter clusters can be seen in the Himalayan, HinduKush and Sulaiman ranges, and in Makran and Bhuj regions, indicating potential seismic sources for potential future earthquakes. Of these earthquakes, the 2005 Kashmir earthquake caused major damage in Pakistan.

The 2005 Kashmir earthquake exposed the poor seismic quality of structures and their inefficient seismic design, and soon after it, new seismic

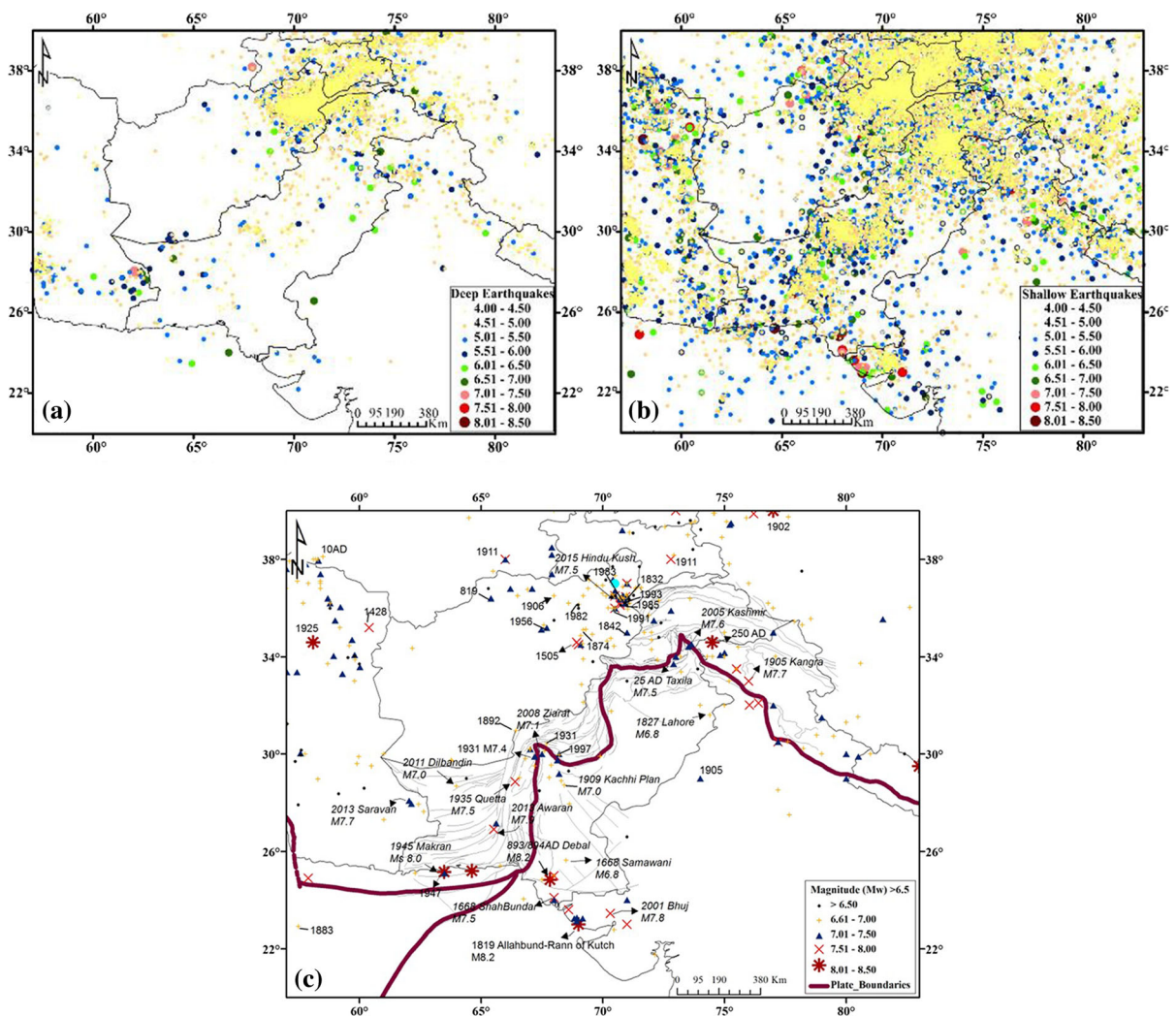


Figure 1

Earthquake catalogue used in the study: **a** epicenters with focal depth up to 50 km; **b** epicenters with focal depth greater than 50 km; **c** epicenters of earthquakes greater than magnitude  $> 6.5$  (Khan et al. 2018)

provisions were introduced as the Building Code of Pakistan in 2007 (BCP 2007) by the Ministry of Housing and Society of Pakistan. The BCP regulations (2007) have been adopted from the Uniform Building Code (UBC 1997), and the seismic hazard zoning map of Pakistan in this regulation was obtained through probabilistic seismic hazard analysis (PSHA) based on the Cornell–McGuire (Cornell 1968; McGuire 1976) approach. The seismic hazard map divides Pakistan into five regions based on peak ground acceleration (PGA) values for flat-rock site conditions having 10% probability of exceedance in 50 years. In the BCP (2007), ground motion prediction equations (GMPEs) developed for shallow crustal regions have been adopted outside and used in the analysis, including the Makran interface subduction region. The choice is inappropriate for the interface subduction according to the Cotton et al. (2006) and Bommer et al. (2010) criteria. The other details about the completeness analysis of the earthquake catalogue that has implications on the earthquake activity rates of seismic sources have not been documented in the BCP (2007). Also, earthquakes with focal depth greater than 70 km have not been considered in the assessment. These characteristics of the BCP (2007) call for attention and evaluation of expected ground motion values in Pakistan through an independent PSHA.

### 3. Probabilistic Seismic Hazard Analysis

In general, to carry out the PSHA using the Cornell (1968) and McGuire (1976) approach, the following elements are required: (1) reliable earthquake catalogue, (2) seismotectonic model, (3) GMPEs and (4) numerical code for the execution of the analysis.

#### 3.1. The Earthquake Catalogue

Earthquake catalogue compilation is the starting point in seismic hazard analysis study, and a reliable catalogue is required for the estimation of seismic hazard. A homogenized, composited and updated earthquake catalogue has been used from the recent study of Khan et al. (2018), which is the initial part of

this study. This catalogue (bounded by geographical region  $57^{\circ}$ – $83^{\circ}$  N and  $20^{\circ}$ – $40^{\circ}$  E) has been compiled by consulting all the available online databanks and individual catalogues available in the literature. It consists of 365,666 events (25 AD – 2016 time span) with lower threshold magnitude  $M_w = 4.0$ . The distribution of the catalogue with respect to the focal depth shows that deep earthquakes are mostly concentrated in the northwest of Pakistan and that shallow earthquakes are distributed in and around the Pakistan territory. In order to differentiate between shallow and deep earthquakes, a focal depth of 50 km is taken as the dividing value for defining the source model for Pakistan (Fig. 2). Individual focal depths for zones are computed and used in the analysis.

The earthquake catalogue has been processed to make it suitable for the Poissonian process assumption of the classical approach. Dependent events (i.e., foreshocks and aftershocks) are removed from the catalogue. Earthquakes falling within the geographical boundaries of the seismic sources are subjected to this operation. This check has been performed in the ZMAP software package (Wiemer 2001) using the algorithm of Gardner and Knopoff (1974). This algorithm has been developed for Southern California and assumes spatial and temporal distribution of fore- and aftershocks as a function of the magnitude of the main shock. This algorithm has also been used in the previous studies for Pakistan (e.g., BCP 2007; Rafi et al. 2012; Waseem et al. 2018b; Zaman et al. 2012). The declustered catalogue superimposed on source zones is shown in Fig. 3a, b.

After the declustering operation, 6765 events were left in the catalogue. The subsequent check for completeness was performed for the catalogue by following the procedures of Mulargia and Tinti (1985) and Stepp (1973). In order to carry out the completeness analysis, all the independent earthquakes were divided into magnitude bins of 0.5 units (e.g., 4.0, 4.5, 5.0, 5.5, 6.0, etc.). Results of the completeness analyses are shown in Figs. 4 and 5. In the Mulargia and Tinti (1985) procedure, the decision on the completeness period is cumbersome (Sesetyan et al. 2018a), and therefore the results obtained using the Stepp (1973) procedure have been used. These results show that, in the earthquake catalogue, the earthquake magnitude range from  $4.0 \leq M_w < 4.5$  is

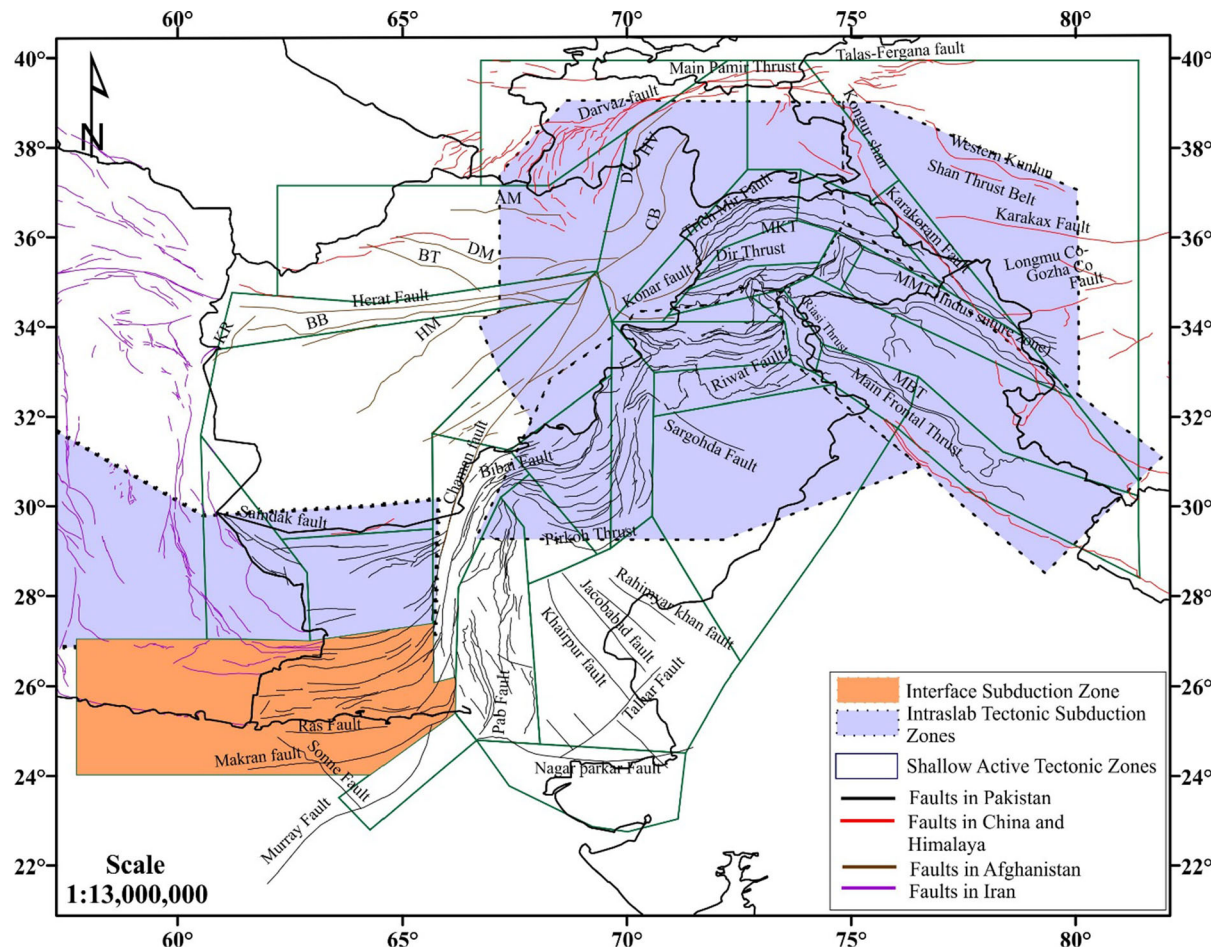


Figure 2  
Seismotectonic model (source model) of Pakistan considered in the PSHA

complete for 1991–2016;  $4.5 \leq M_w < 5.0$  (1971–2016);  $5.0 \leq M_w < 5.5$  (1961–2016);  $5.5 \leq M_w < 6.0$  (1926–2016);  $6.0 \leq M_w < 6.5$  (1876–2016);  $6.5 \leq M_w < 7.0$  (1866–2016) and for  $M_w$  greater than and equal to 7.0 in 1826–2016. The  $4.0 \leq M_w < 4.5$  magnitude range has a completeness period of 1991–2016, whereas  $4.5 \leq M_w < 5.0$  is completed for 1971–2016. It is observed that the period 1971–2016 also covers the 1991–2016 period, and the catalogue is completed from 1971 (i.e.,  $4.0 \leq M_w < 5.0$ ). Similarly, the 1971–2016 period is covered by the completeness period of  $5.0 \leq M_w < 5.5$  (i.e., 1961–2016), and hence the catalogue is completed for all earthquakes in the range of  $4.0 \leq M_w < 5.5$  since 1961. Similarly,  $M_w \geq 7.0$

covers the period 1826–2016 for all earthquakes in catalogue, and thus the earthquake catalogue is completed for 1826–2016. This fact is further explained in Fig. 6.

In the catalogue, the historical events from Khan et al. (2018) have been compiled from the studies of Oldham (1883), Quittmeyer and Jacob (1979), Bilham (1999), Ambraseys (2000), Ambraseys and Bilham (2003, 2009), Ambraseys and Douglas (2004), Bilham and Ambraseys (2005), Bilham et al. (2007), Heidarzadeh et al. (2008) and Martin and Szeliga (2010).

Completeness periods of magnitudes are used to compute the annual rate of exceedance of earthquakes to obtain the recurrence relationships.

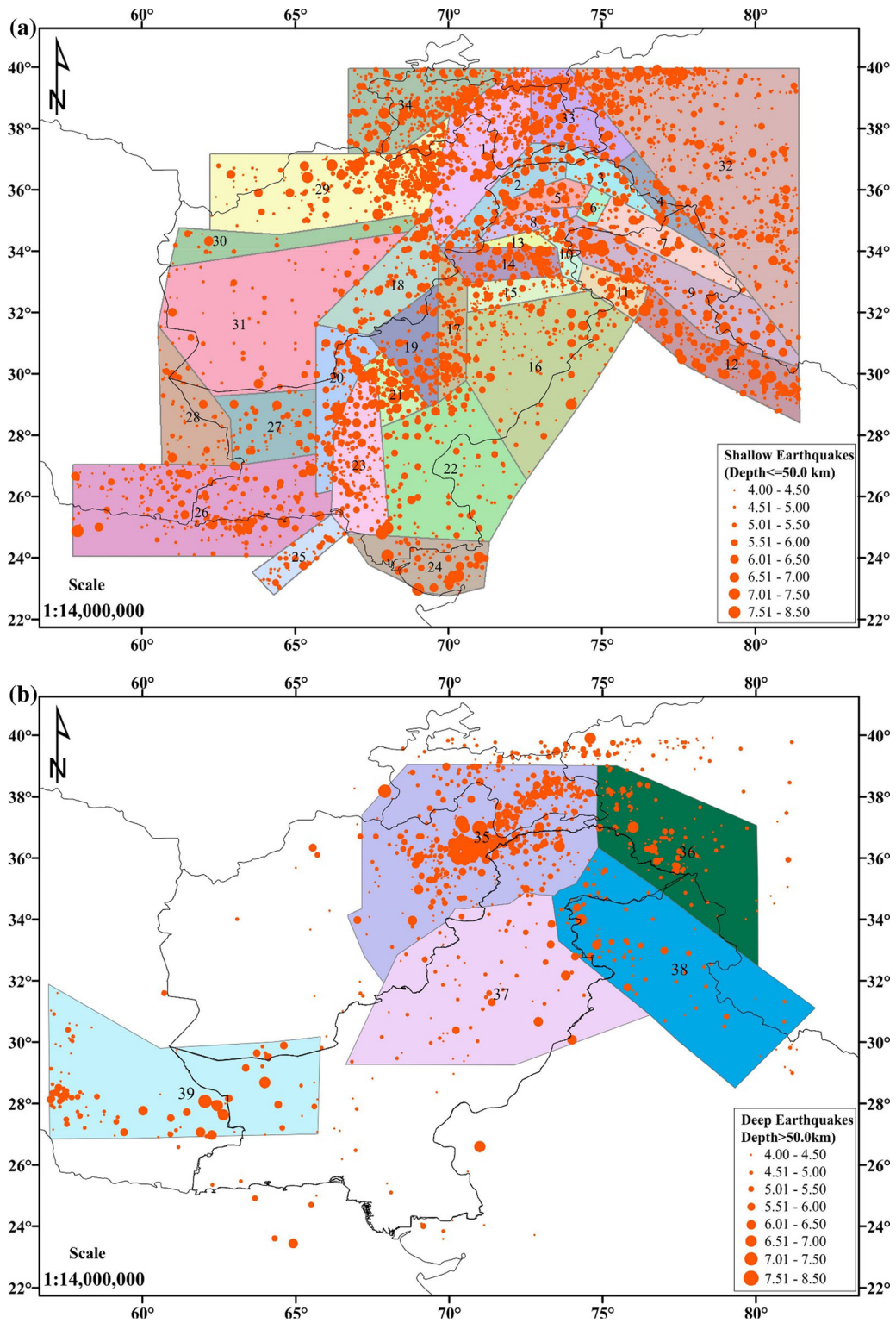


Figure 3  
a Shallow source model in the study. b Deep source model in the study

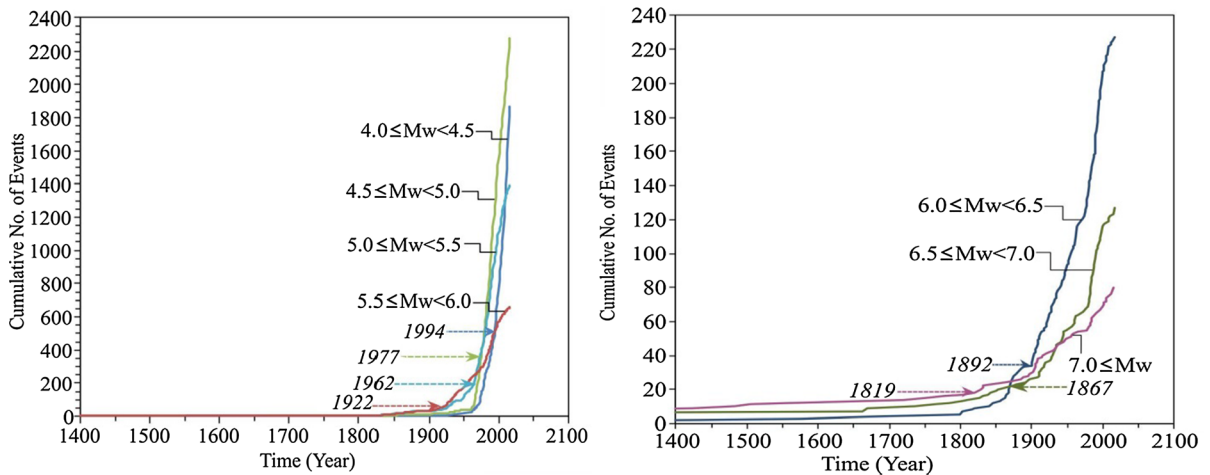


Figure 4  
Completeness analysis of the declustered catalogue by the Tinti and Mulargia (1985) method

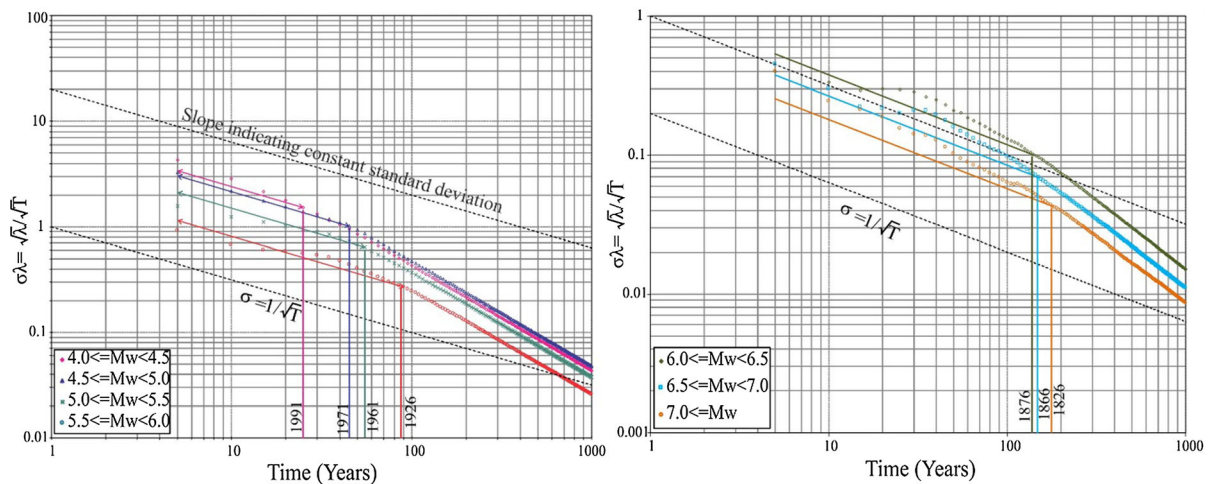


Figure 5  
Completeness analysis of the declustered catalogue results by the Stepp (1973) method

### 3.2. Source Model

In order to use the classical Cornell (1968) approach, a source model (seismic source zones) is required as important input for the analysis. In the source model, potential seismic zones are delineated using information on the tectonics and earthquake seismicity pattern and active faults. The complete source model for the study area is presented in Fig. 2 where tectonic regions of active shallow crustal, interface subduction and deep seismicity associated

with the dipping slab exist. This model consists of 34 shallow and five deep source zones. In southern Pakistan, source zones are updated from Waseem et al. (2019). The source model is characterized by overlapped areas. Active shallow source zones are associated with seismicity up to 50 km, and deep source zones are associated with seismicity greater than 50 km. Deep seismicity is associated with the dipping intraslab subduction in the HinduKush, Karakorum and Himalayan region. The deep

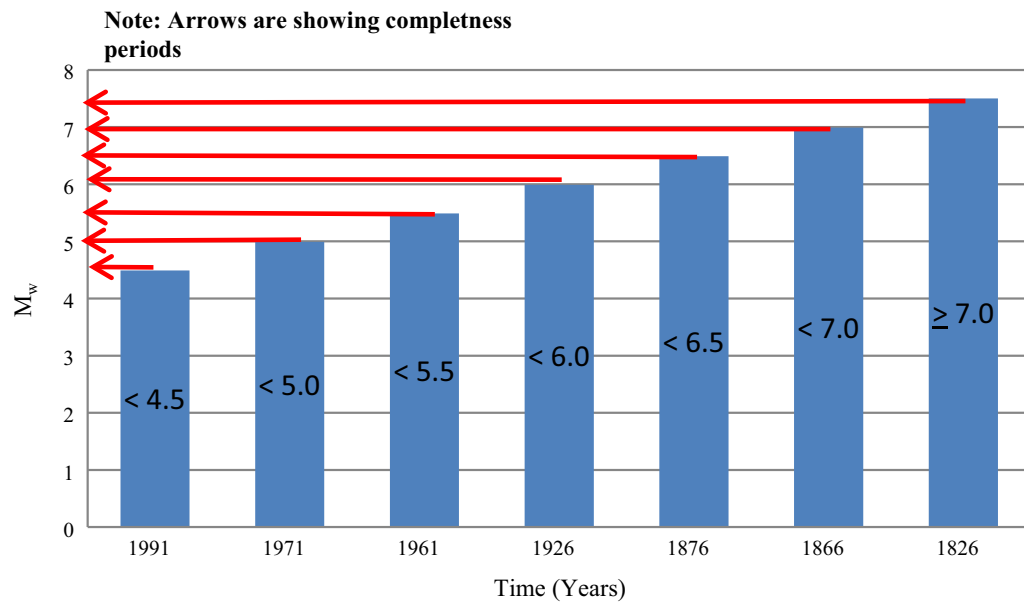


Figure 6  
Completeness of the earthquake catalogue

seismicity source model is overlaid on the active shallow source zones. Expert judgment is used to define the boundaries of the source zones: seismically high active regions have been separated from the low-seismicity regions, provided that they are supported by well-defined active faults. Since marked faults were not available, seismicity patterns and expert judgment are used in the delineation of the deep seismicity source zone. Expert judgment used in delineation of the seismic source model can be summarized in following two points:

1. When both seismicity and geological information are available, geological information has been used to separate the two adjacent source zones. For example, the Himalayan is separated from the Kohistan Island Arc. Similarly, the HinduKush ranges and Karakorum ranges are separated, and so on.
2. When seismicity data was limited, geological information of an area has been used in defining the boundary and shape of the seismic source zone.

The model proposed in this study is dominantly based on active faults of Pakistan and surroundings

(Gulen et al. 2014; Taylor and Yin 2009; Styron et al. 2010). Delineation of source zones is carried out considering major tectonic features located in the region, and a summary of such is presented in the following section.

The Makran shallow active interface subduction zone is located along the south coast of Pakistan and southeast of Iran (source zone 26). The Makran subduction zone represents interaction of Arabian, Eurasian and Indian plates where a major tectonic feature is formed. Seismically, it is moderately active. The Makran region experienced the 1945 Makran coast earthquake of  $M$  8.2 (that caused a tsunami) and the recent 2011 Dalbandin earthquake of  $M$  7.2.

Another very prominent tectonic feature in the south of Pakistan is known as the Chaman fault system, located in the displacement region between the Indian plate and Helmand block with a fault length greater than 850 km (i.e., source zone 20). The Chaman fault is a moderately active left-lateral strike-slip transform fault with a slip rate of 9–24 mm/year (Lawrence et al. 1992). Most of the differential movement between the Eurasian and Indian plates is accommodated by the Chaman fault. The Chaman fault has ruptured twice, first in 1505



and then in 1892 (Quittmeyer and Jacob 1979). The Chaman fault is trending northwest to northeast and it finally meets the right-lateral Herat fault where it merges with the Pamir fault system in Afghanistan. It has been divided into two zones based on its trend (a portion of the Chaman fault entering Afghanistan is a separate zone). The right-lateral strike-slip Herat fault is not very active and is running in the east–west direction in Afghanistan. The Ornach–Nal fault is another strike-slip fault that forms the eastern margin of the Makran region and is characterized by diffused seismicity, often taken as part of the Chaman fault.

The Sulaiman and Kirthar ranges are part of the Sulaiman and Kirthar fold-and-thrust belt formed by the Indian and Eurasian plates, located in southern Pakistan beside the Chaman fault systems in the western side. The Sulaiman range is seismically very active and is where the 1935 Quetta earthquake occurred. On the other hand, the Kirthar range is not as active as the Sulaiman range. In this study, separate source zones have been drawn for these two ranges.

The Rann of Kutch in the southeast of Pakistan is also a potential source of the 2001 Bhuj earthquake of  $M$  7.7 and the 1819 Rann of Kutch earthquake. This region is considered as one seismic source zone in this study. In this zone, the major tectonic activities are due to the east–west-trending Nagar Parkar strike-slip fault. This zone has been separated from the Indian shield zone which has Khairpur, Rahimyar Khan and Talhar faults. Punjab plains lying in the vicinity of the Indus basin are considered as different zone where the Sargodha fault is located. The Indus basin and Punjab plain have been separated into two source zones, perhaps due to the presence of active faults; a much-diffused seismicity has been noted as compared to other regions.

The Kohistan island arc is located in the north-western region of Pakistan bordered by the Main Karakorum Thrust (MKT) and Main Mantle Thrust (MMT). It is an extension of Pamir–HinduKush mountain ranges and covers shallow- and intermediate-focused earthquakes (Mukhopadhyay and Dasgupta 2015). Characteristically, this island arc has low seismicity. Only one major earthquake of  $M$  6.0 near Gilgit had occurred. In source zone 6, the Nanga Parbat syntaxis, which formed at the northeast

of the MKT, has a sharp transformation. Similar to the Nanga Parbat syntaxis, there also exists the Hazara Kashmir syntaxis where the Main Boundary Thrust (MBT) changes its orientation. The Nanga Parbat syntaxis and Hazara Kashmir syntaxis are considered in separate source zones from their adjoining structures. Beyond the MKT, in the north-west and north, mountain ranges of Karakorum and Pamir are located within the plate boundary of the Eurasian plate. The Kohistan Island arc, HinduKush-Pamir and Karakorum form separate source zones. The Ladakh arc is bounded by the MMT in the north and by the Karakorum strike-slip fault in the east. The Karakorum fault is a strike-slip fault dividing the features among the Tibetan plateau, Pamir and Tibetan–Himalayan. In source zone 7, the Ladakh arc has been separated from the Nanga Parbat syntaxis (source zone 6) and Karakorum ranges.

In the northeast of Pakistan, the world's most active Karakorum and HinduKush–Pamir regions are located. These regions represent interaction of the Eurasian and Indian plates where intermediate and deep-focus earthquakes are very common (Waseem et al. 2018a). The Himalayan fold-and-thrust belt, an extensive collision belt, is also formed in northern Pakistan. Northern Pakistan has been divided by Gansser (1981) into (1) sub-Himalayan located between the Himalayan Frontal Thrust (HFT) and Main Boundary Thrust (MBT); (2) lesser Himalayan bounded in the north by the Main Central Thrust (MCT) and MBT in the south; (3) higher Himalayan between the MCT and Main Mantle Thrust (MMT); (4) Tethayan Himalayan located in the north of Higher Himalayan and MMT; (5) Indus–Tsangpo suture zone; and (6) Indian shield and Punjab plain. Two important strike-slip faults are formed in the Lesser Himalayan: (1) left-lateral Jhelum fault and (2) right-lateral strike-slip Kalabagh fault which form the left margin of the HFT. The Jhelum fault is an active fault along which Hazara, Murree and Abbotabad formations are highly deformed (Baig and Lawrence 1987). The Kalabagh fault forms the right margin of the HFT, which separates the Potwar and Kohat Plateau. The Himalayan is separated from Kohistan island arc and other tectonic entities, and the major thrust divisions have been used to define seismic zones.

The deep source model considered in the analysis is originally selected from work of Waseem et al. (2018b) for northern Pakistan, and one additional deep seismicity source zone is defined in the south of Pakistan.

### 3.3. Source Characterization

The source model zones are characterized using the number of earthquakes, by the maximum magnitude potential and by Gutenberg–Richter parameters. The assigned maximum magnitude potential of the zones is estimated by the maximum earthquake that occurred in the source zone plus 0.5 units to account for possible errors in estimation. The fault-based magnitude potential of the zones is also estimated. The Wells and Coppersmith (1994) relationship has been used in order to compute the fault magnitude potential. It has been observed that both approaches yield the magnitude in the same range. Therefore, considering the maximum historic approach for computing the maximum magnitude potential of seismic zones will not lower the hazard level.

### 3.4. Earthquake Recurrence

Gutenberg–Richter recurrence law (1956) is established for each seismic source zone using the processed earthquake catalogue. The number of earthquakes in each source zone after performing the declustering and completeness is used to derive the Gutenberg–Richter (1956) recurrence law. It is obtained for all the defined seismic sources by carrying out least square regression analysis on the logarithm of cumulative number of earthquakes and their magnitude values present in the source zones. The standard Gutenberg–Richter recurrence law covers an infinite range of magnitude (Kramer 1996). Therefore, a truncated Gutenberg–Richter recurrence law is also obtained to estimate the expected earthquake magnitude. The truncated law formulation is given by the following expression (1):

$$\lambda = v_0 \cdot \frac{\exp^{-\beta \cdot (M_w - M_w^{\min})}}{1 - \exp^{-\beta \cdot (M_w^{\max} - M_w^{\min})}}, \quad (1)$$

where  $v_0 = \exp(\alpha - \beta \cdot M_w^{\inf})$ ,  $M_w^{\min}$  and  $M_w^{\max}$  are lower and upper bounds of moment magnitude  $M_w$ .

The Gutenberg–Richter law is truncated at the minimum magnitude of engineering importance ( $M_w = 4.0$ ) and maximum magnitude value observed plus 0.5 units. Minimum magnitude is chosen on the basis of the minimum magnitude that will cause damage. Plots of the Gutenberg and Richter recurrence relationships are shown in the Appendix 1, and the source parameters for each zone are reported in Table 1. The individual completeness periods ( $4.0 \leq M_w < 4.5$ , 1991–2016;  $4.5 \leq M_w < 5.0$ , 1971–2016, etc.) have been used in the computation of the Gutenberg–Richter recurrence laws.

The reported parameters include number of earthquakes in zones, lower and upper limits on magnitude, Gutenberg and Richter parameters “ $a$ ,  $b$ ,  $\alpha$ , and  $\beta$ ”. The  $a$  value represents the total seismicity of the source and  $b$  value is representing the ratio and large to small magnitude potential and its value is close to 1.0 for seismically active zones. A smaller  $b$  value of zone implies potential for large future earthquakes in that zone. In this work, zone 15, 17, 19, 23, 25 and 36 have  $b$  values greater than 1.0 and the rest of the zones have  $b$  values less than 1.0. Only Zone 24 has lowest  $b$  value of 0.703.

### 3.5. Ground motion prediction equations

GMPEs are also one of the essential elements in the seismic hazard computations which predict ground motion intensities for different levels of exceedance rate. PGA values are region-specific and require a dense network, so, first, the GMPEs developed based on local data are preferred. A robust GMPE development based on the indigenous data-bank of Pakistan is still not available. Shah et al. (2012) presented the only GMPE for Pakistan developed based on a local dataset of shallow earthquakes in northern Pakistan. The work of Shah et al. (2012) has been developed for predicting the PGA values, and it is not feasible to use it in the PSHA due to two reasons, as per the recommendations of Cotton et al. (2006): (1) it has not been developed using standard regression analysis procedures (e.g., Joyner and Boore 1981; Fukushima and Tanaka 1990); (2) it is not published in an international peer-reviewed journal; and (3) additionally, the standard deviation of the GMPE is also not provided using which

Table 1  
 Characteristics of seismic sources

Source zone	N	$a$ value	$b$ value	" $v_0$ "	$\alpha$ value	$\beta$ value	$M_{\min}$	$M_1$	$M_2$	$M_{\max}$
1	402	5.237	0.987	19.467	12.061	2.273	4.0	7.8	7.8	7.8
2	120	4.343	0.890	6.066	10.001	2.049	4.0	7.9	7.4	7.9
3	60	4.443	0.974	3.509	10.232	2.244	4.0	6.9	7.4	6.9
4	58	3.106	0.714	1.781	7.152	1.644	4.0	8	7.7	8.0
5	57	3.162	0.725	1.834	7.282	1.669	4.0	7.9	6.9	7.9
6	17	3.002	0.800	0.634	6.914	1.842	4.0	6.9	7.0	6.9
7	64	4.375	0.951	3.726	10.076	2.190	4.0	7.2	7.0	7.2
8	52	3.553	0.808	2.087	8.183	1.862	4.0	7.4	7.1	7.4
9	241	4.398	0.858	9.274	10.129	1.975	4.0	9.0	7.9	9.0
10	48	2.951	0.717	1.025	6.796	1.651	4.1	8.0	6.9	8.0
11	57	4.253	0.940	3.108	9.795	2.165	4.0	7.0	7.2	7.0
12	260	4.418	0.855	10.000	10.175	1.968	4.0	8.2	7.8	8.2
13	17	2.649	0.775	0.354	6.101	1.785	4.0	6.2	6.9	6.2
14	164	4.156	0.858	5.320	9.572	1.975	4.0	8.0	7.5	8.0
15	89	5.173	1.126	4.650	11.913	2.594	4.0	7.1	7.6	7.1
16	207	4.776	0.962	8.468	10.998	2.215	4.0	7.6	7.4	7.6
17	150	5.103	1.041	8.731	11.753	2.396	4.0	7.5	7.6	7.5
18	125	4.048	0.847	4.558	9.323	1.951	4.0	8.2	7.8	8.2
19	107	5.167	1.082	6.892	11.900	2.492	4.0	7.3	7.2	7.3
20	121	3.671	0.758	3.660	8.454	1.745	4.1	8.2	7.8	8.2
21	112	3.536	0.736	3.893	8.143	1.696	4.0	8.0	8.1	8.0
22	127	4.860	0.997	7.419	11.193	2.297	4.0	6.9	7.6	6.9
23	218	5.296	1.048	12.705	12.196	2.413	4.0	8.7	8.1	8.7
24	78	3.099	0.703	1.945	7.137	1.618	4.0	8.7	7.7	8.7
25	48	5.113	1.139	2.766	11.775	2.624	4.1	6.6	7.5	6.6
26	270	3.677	0.702	7.404	8.467	1.616	4.0	8.7	7.5	8.7
27	62	4.252	0.941	3.081	9.793	2.167	4.0	7.1	7.3	7.1
28	65	3.739	0.846	2.259	8.610	1.949	4.0	7.3	7.3	7.3
29	383	4.736	0.887	15.407	10.906	2.043	4.0	8.0	7.8	8.0
30	35	4.028	0.962	1.518	9.276	2.215	4.0	7.3	7.6	7.3
31	81	4.338	0.950	3.456	9.992	2.188	4.0	7.5	7.3	7.5
32	706	5.506	0.987	36.091	12.680	2.273	4.0	8.2	7.9	8.2
33	214	4.284	0.836	8.685	9.866	1.926	4.0	8.1	7.7	8.1
34	371	4.959	0.942	15.566	11.419	2.168	4.0	7.8	7.8	7.8
35	626	4.209	0.733	18.925	9.694	1.688	4.0	8.4	–	8.4
36	118	5.373	1.141	4.971	12.373	2.627	4.1	7.2	–	7.2
37	67	3.865	0.875	2.316	8.900	2.015	4.0	7	–	7.0
38	76	4.325	0.969	2.254	9.961	2.231	4.1	7.2	–	7.2
39	109	3.762 $M_2$ = maximum observed magnitude + 0.5 unit; $M_3$ = fault-based magnitude potential	0.795	3.179	8.664	1.831	4.1	8.0	–	8.0

$M_2$  maximum observed magnitude + 0.5 unit,  $M_3$  fault-based magnitude potential

variation in ground motion is considered in the PSHA.

The findings of Shah et al. (2012) are considered inappropriate and lack a robust GMPE; thus, we are left with the choice of adopting the GMPEs from outside regions.

The criterion set for adopting GMPEs in this study is that worldwide accepted global GMPEs developed for similar tectonic settings of the host regions may be used in the analysis, which can predict both PGA and spectral acceleration (SA) intensity values.

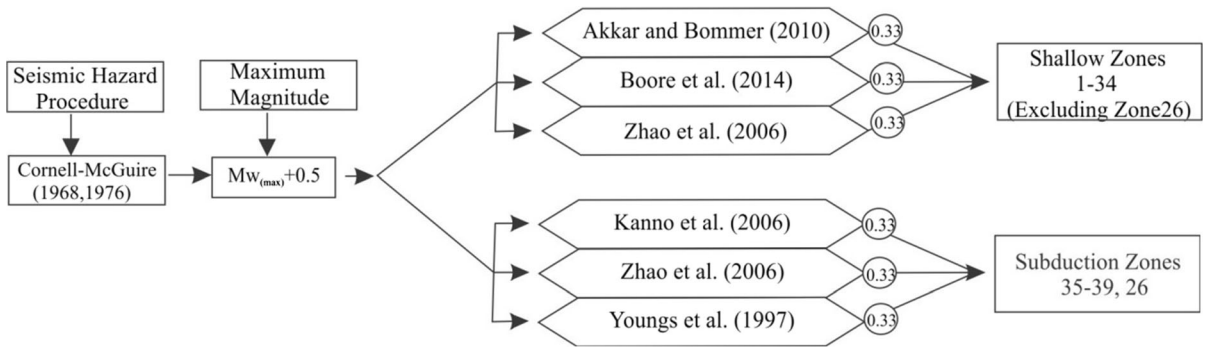


Figure 7  
Logic tree used in the study

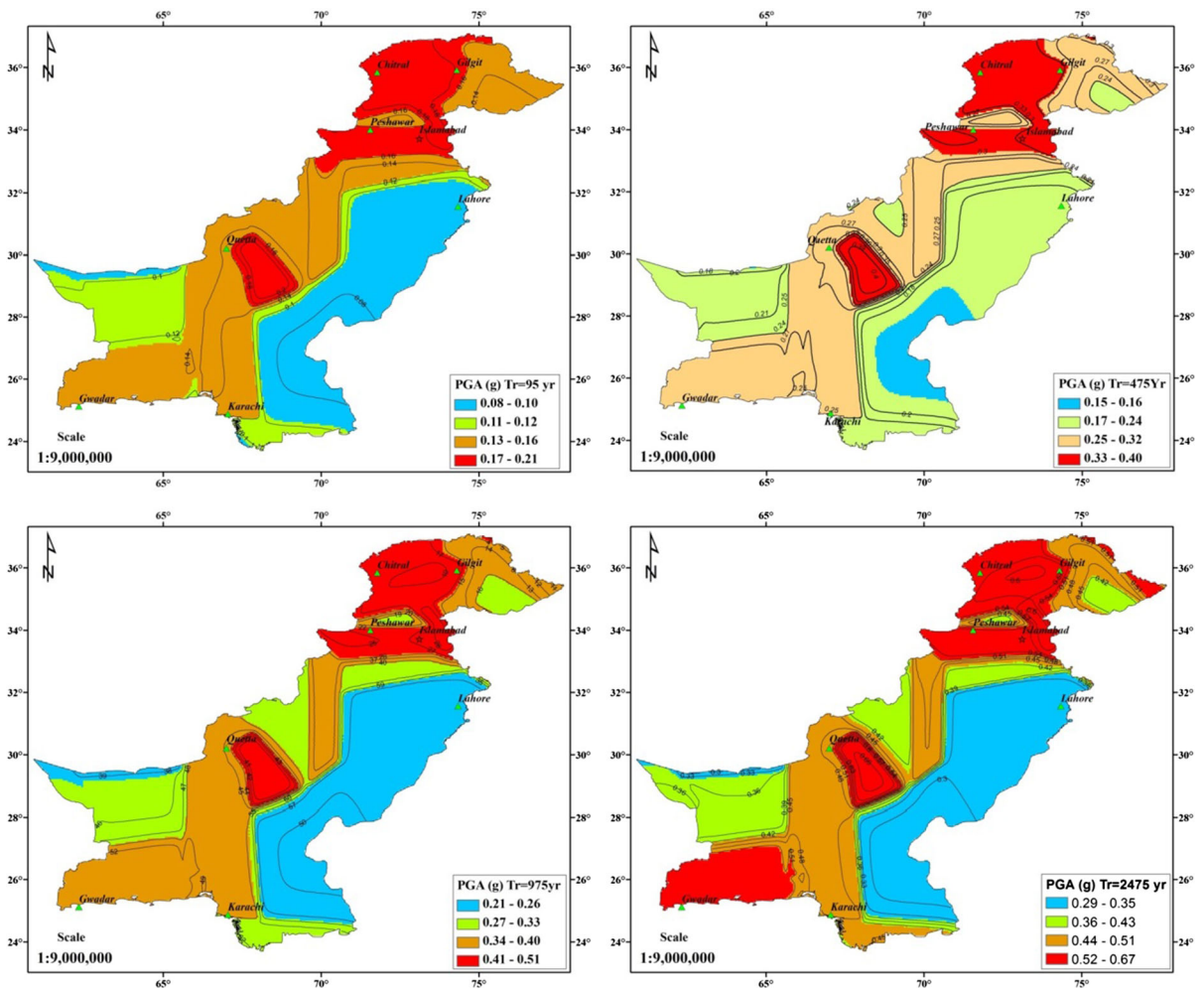


Figure 8  
Seismic hazard maps of Pakistan in terms of PGA for different return periods

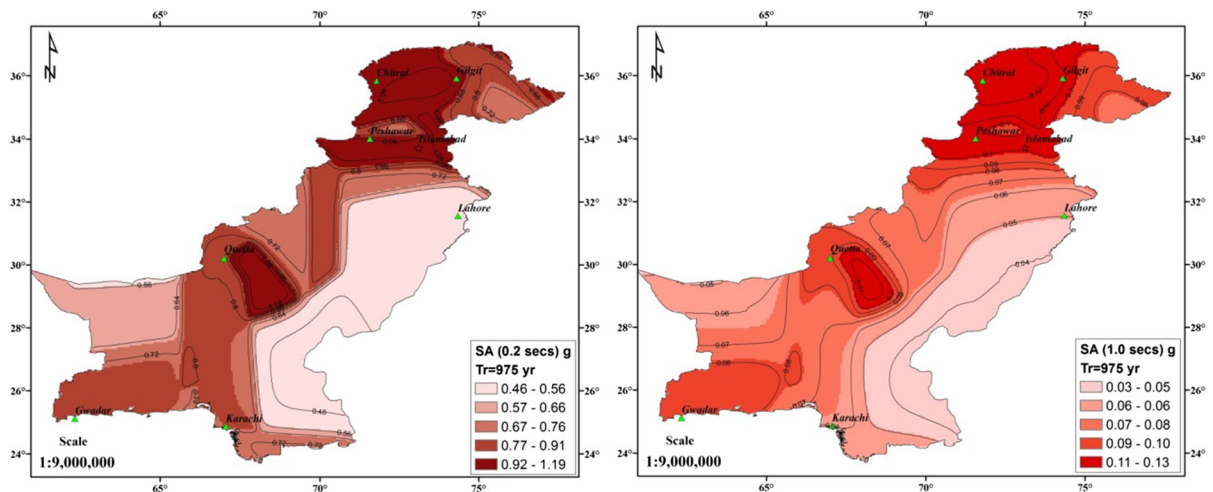


Figure 9  
Seismic hazard maps of Pakistan in terms of SA at 0.2 s and 1.0 s for the 975-year return period

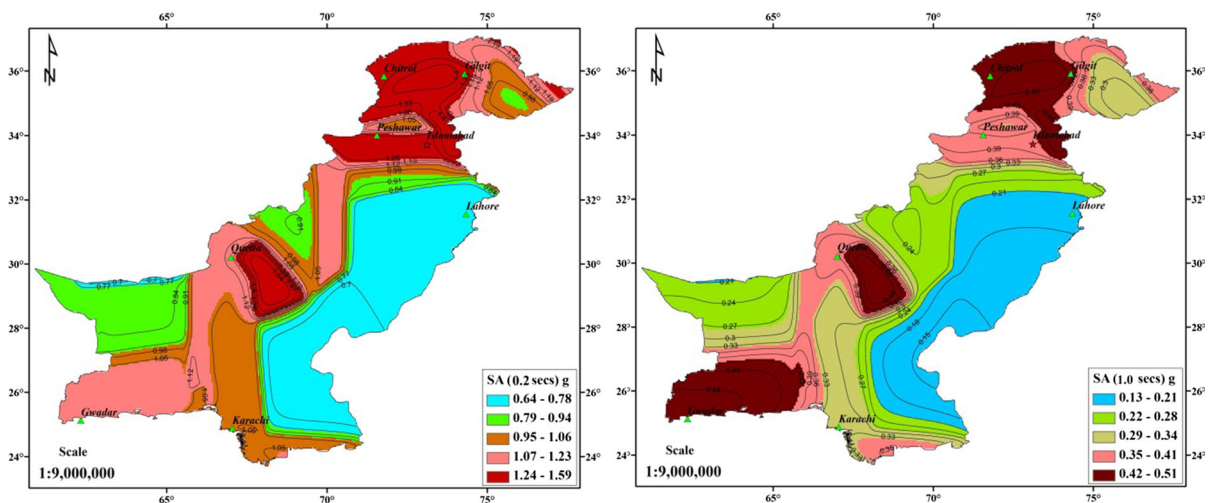


Figure 10  
Seismic hazard maps of Pakistan in terms of SA at 0.2 s and 0.1 s for the 2475-year return period

Three broad tectonically unique settings exist in the study region: (1) interface subduction present in the southwestern coast (Makran subduction zone); (2) deep crustal earthquakes in HinduKush and Pamir in the northwest of Pakistan and Himalayan and Karakorum regions in northeast of Pakistan; and (3) shallow crustal regions including the Chaman, Sulaiman, Kirthar and Himalayan regions. Therefore, three distinct types of GMPEs are required to perform the computations.

Three GMPEs, i.e., Akkar and Bommer (2010), Boore et al. (2014), and Zhao et al. (2006), are used for shallow earthquakes, and three equations (i.e., Zhao et al. 2006; Youngs et al. 1997; Kanno et al. 2006) are used for subduction interface and deep crustal earthquakes. These GMPEs are selected randomly, and more than one GMPE is used for each tectonic region. Intra-slab subduction GMPEs are considered applicable in the deep crustal earthquake regions. The Akkar and Bommer (2010)

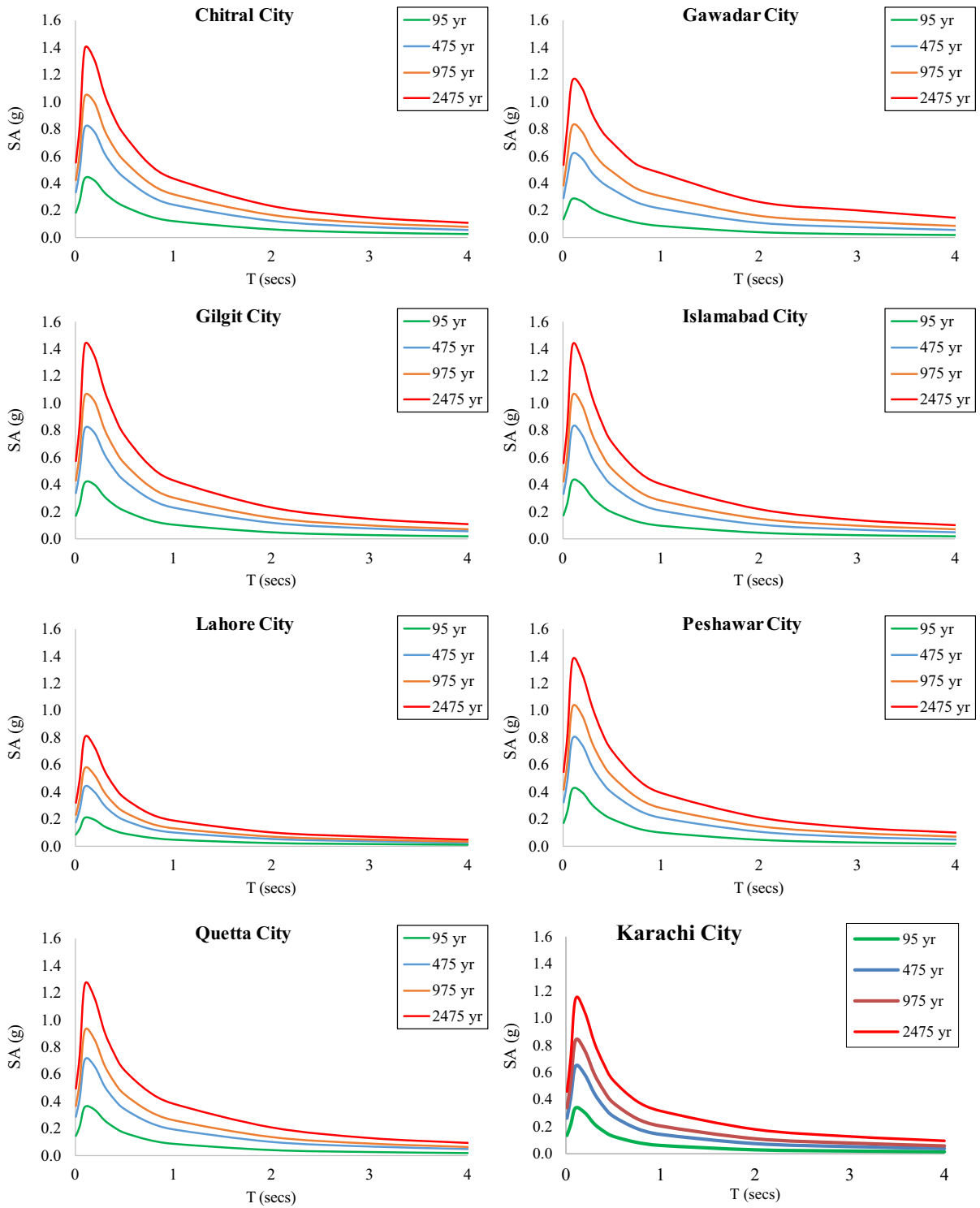


Figure 11  
Uniform hazard spectra (UHS) obtained for important cities in Pakistan

Table 2

*Ground motion values for different cities obtained in the current study*

S. no	City	PGA (g) for 95-, 475-, 975- and 2475-year return periods				SA (g) for the 975-year return period		SA (g) for the 2475-year return period	
		95 years	475 years	975 years	2475 years	0.2 s	1.0 s	0.2 s	1.0 s
1	Chitral	0.18	0.33	0.42	0.55	0.99	0.32	1.30	0.44
2	Gilgit	0.18	0.34	0.44	0.58	1.03	0.31	1.37	0.44
3	Naran	0.18	0.33	0.42	0.56	0.99	0.30	1.32	0.43
4	Batakhundi	0.17	0.31	0.40	0.53	0.94	0.29	1.25	0.41
5	Balakot	0.19	0.36	0.46	0.61	1.07	0.32	1.42	0.46
6	Muzaffarabad	0.18	0.35	0.45	0.60	1.06	0.32	1.42	0.46
7	Mansehra	0.15	0.28	0.35	0.47	0.84	0.27	1.13	0.38
8	Abbottabad	0.16	0.29	0.37	0.49	0.88	0.28	1.18	0.39
9	Islamabad	0.18	0.33	0.42	0.56	0.98	0.28	1.30	0.40
10	Peshawar	0.17	0.33	0.41	0.55	0.96	0.28	1.27	0.39
11	DI Khan	0.10	0.19	0.24	0.33	0.56	0.15	0.76	0.21
12	Lahore	0.09	0.18	0.23	0.32	0.53	0.13	0.73	0.19
13	DG Khan	0.11	0.21	0.27	0.36	0.62	0.15	0.84	0.21
14	Chaman	0.13	0.27	0.35	0.47	0.79	0.24	1.09	0.36
15	Quetta	0.15	0.29	0.37	0.50	0.85	0.26	1.16	0.39
16	Jacobabad	0.11	0.21	0.27	0.37	0.65	0.19	0.89	0.28
17	Hyderabad	0.09	0.17	0.22	0.31	0.51	0.14	0.71	0.22
18	Karachi	0.13	0.26	0.34	0.46	0.76	0.20	1.04	0.31
19	Gwadar	0.14	0.29	0.39	0.54	0.78	0.31	1.10	0.48

equation is preferred over its latest version of Akkar et al. (2014) due to its robust performance in the study of Waseem et al. (2018b). All the selected GMPEs are well accepted and have been used worldwide in seismic hazard assessment studies.

#### 4. Epistemic Uncertainties

Epistemic uncertainties in the seismic hazard assessment procedure are inherent in the process due to lack of knowledge about earthquakes and generation of the ground motion process. These uncertainties are addressed by using a logic tree, where each branch of the logic tree represents decision step confidence of the analyst (Sesetyan et al. 2018a). Branches of a logic tree are usually related to the GMPEs, source models and their characterization. The logic tree implemented in the analysis has 12 branches, and it has been constructed only for the GMPEs in the current study. Each attenuation equation on the logic tree is given equal weight to capture equally the uncertainties in the assessment. The weights are kept equal because all of the GMPEs are

well accepted and have been used throughout the world. Three GMPEs each have been used for deep sources and shallow sources. The logic tree adopted in this study is shown in Fig. 7. Each GMPE has been assigned 0.33 on the logic tree.

#### 5. Results and Discussions

This study seismic hazard assessment for Pakistan is carried out in a  $0.1^\circ$  rectangular grid and to obtain spatial distribution of ground motion for intensity parameters, mean PGA and 5% damped mean SA at  $T = 0.2$  and  $T = 1.0$  s. The analysis is carried out in the EZ-FRISK 7.62 version developed by Risk International. In order to perform PSHA in EZ-FRISK, information on the basic elements is required. Characteristics (maximum expected magnitude, activity rate, geometry) of every source zone are needed. GMPEs are assigned to zones, and their weights are assigned on the logic tree. The ground motion intensity parameters are specified, and the levels of intensity parameters are identified on a seismic hazard curve. The following expression (2) is

Table 3

Contribution of deep earthquakes for 475- and 2475-year return periods

S. no	City	PGA values due to deep and shallow earthquakes	PGA values due to deep earthquakes only	Contribution of deep earthquakes (%)
475-year return period				
1	Chitral	0.33	0.21	63.63
2	Gilgit	0.34	0.17	63.64
3	Naran	0.33	0.15	50.00
4	Batakhundi	0.31	0.15	45.45
5	Balakot	0.36	0.14	48.39
6	Muzaffarabad	0.35	0.12	38.89
7	Mansehra	0.28	0.12	34.29
8	Abbottabad	0.29	0.12	42.86
9	Islamabad	0.33	0.10	41.38
10	Peshawar	0.33	0.13	30.30
11	DI Khan	0.19	0.08	39.39
12	Lahore	0.18	0.07	42.11
13	DG Khan	0.21	0.07	38.89
14	Chaman	0.27	0.06	33.33
15	Quetta	0.29	0.06	22.22
16	Jacobabad	0.21	0.03	20.69
17	Hyderabad	0.17	0.01	14.29
18	Karachi	0.26	0.01	5.88
19	Gwadar	0.29	0.03	3.85
2475-year return period				
1	Chitral	0.55	0.36	65.45
2	Gilgit	0.58	0.32	55.17
3	Naran	0.56	0.28	50.00
4	Batakhundi	0.53	0.27	50.94
5	Balakot	0.61	0.25	40.98
6	Muzaffarabad	0.60	0.22	36.67
7	Mansehra	0.47	0.22	46.81
8	Abbottabad	0.49	0.21	42.86
9	Islamabad	0.56	0.18	32.14
10	Peshawar	0.55	0.23	41.82
11	DI Khan	0.33	0.14	42.42
12	Lahore	0.32	0.12	37.50
13	DG Khan	0.36	0.12	33.33
14	Chaman	0.47	0.10	21.28
15	Quetta	0.50	0.11	22.00
16	Jacobabad	0.37	0.06	16.22
17	Hyderabad	0.31	0.02	6.45
18	Karachi	0.46	0.02	4.35
19	Gwadar	0.54	0.05	9.26

used by the EZ-FRISK to compute the rate of earthquakes:

$$H_{(a)} = \sum v_i \iint P[A > a/m, r] f_{m(M)} \times f_{RM}(r, m) d_r d_m. \quad (2)$$

In the above equation,  $H_{(a)}$  is the annual rate of earthquakes producing earthquake amplitude “ $A$ ” greater than “ $a$ ,” and  $f_{m(M)}$ ,  $f_{RM}$  are probability density functions for earthquake magnitude and distance. “ $v_i$ ” is the annual rate of earthquakes greater than the minimum threshold magnitude in a seismic source, and  $P[A > a/m, r]$  is the probability that an earthquake of magnitude “ $m$ ” at a distance “ $r$ ” at a location produces amplitude “ $A$ ” (e.g., PGA, PGD or PGV, etc.) greater than “ $a$ .”

The summation of rate given by the above equation is extended over the all the seismic sources. The analysis in the current study is truncated at  $+3\sigma$  for every GMPE. The probability that ground motion “ $A$ ” will exceed “ $a$ ” is estimated by the following expression (3) based on the assumption that occurrence of an earthquake process is Poissonian:

$$P[A > a/m, r] = 1 - e^{-H_{(a)}}. \quad (3)$$

From Figs. 8, 9 and 10, we present seismic hazard maps corresponding to the return periods (RPs) of 475, 975 and 2475 years. These maps correspond to the rock site conditions. The color coding in the maps shows amplitude variation of ground motion parameters. Uniform hazard spectra obtained for important cities are shown in Fig. 11.

From the overall evaluation of the spatial distribution of ground motion in Pakistan, we may say that the HinduKush, Kohistan and Sulaiman ranges are characterized by highest hazard in Pakistan territory. The southwestern region, where the Makran subduction zone and Chagai Arc are formed, is characterized by a lower hazard level, i.e., 0.25–0.27 g and 0.17–0.24 g, respectively, for the 475-year RP. The Makran region was not expected to have very high intensity values as it is not as active as the Himalayan thrust fold belt and HinduKush region. Therefore, it was expected, and the results complement it. The left-lateral strike-slip Chaman fault system (with slip rate of 9–24 mm/year) located adjacent to the Makran region and Kirthar ranges is observed as being hazardous compared to its portion in Afghanistan. The Indian shield region has been observed as the lowest hazard zone in Pakistan, as expected, because it was characterized by diffused seismicity.



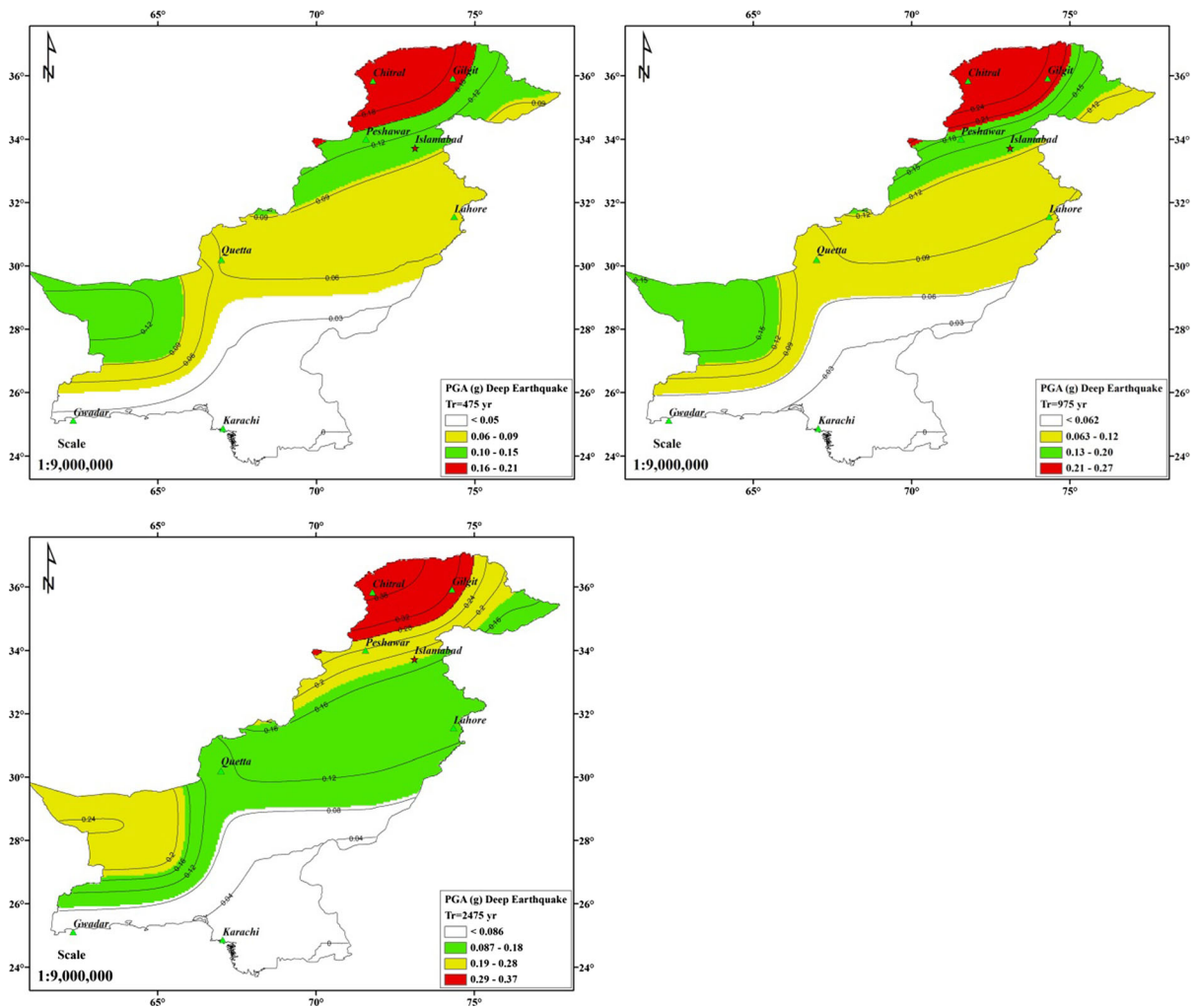


Figure 12

Seismic hazard of Pakistan due to deep earthquakes for 475-, 975- and 2475-year return periods

PGA corresponding to 475 years has been the standard parameter used by seismic hazard studies in Pakistan, and the PGA results of this study have been compared with previous studies. It has been observed that the maximum PGA value obtained in this study is 0.40 g which is greater than the values of the BCP (2007) study and less than the Sesetyan et al. (2018b) study. Lower PGA values obtained in this study may have resulted due to selection of the area source model, while Sesetyan et al. (2018b) used a hybrid model of the area and fault sources. This study is not directly comparable to Sesetyan et al. (2018b) and Zaman et al. (2012) due to difference in the source

models and hazard approach. But it is comparable with the Global Seismic Hazard Assessment Program (GSHAP) (Zhang et al. 1999), BCP (2007) and Rafi et al. (2012) seismic hazard models. A higher level of ground motions is observed in the current study as compared to Rafi et al. (2012) and Zhang et al. (1999). Higher ground motion values are due to usage of an updated and more complete earthquake catalogue and recent GMPEs in the analysis.

Seismic hazard maps corresponding to SA obtained in this study provide definition of the hazards consistent with IBC (2015) and AASHTO (2012) guidelines. The resulted maps show that ground

Table 4

Comparison of PGA values for a 475-year return period estimated in BCP (2007) and in the current study

S. no	City	PGA values for 475 years in current study (g)	PGA value for 475 years in BCP (2007) (g)
1	Chitral	0.33	> 0.32
2	Gilgit	0.34	0.24–0.32
5	Balakot	0.36	> 0.32
6	Muzaffarabad	0.35	> 0.32
8	Abbottabad	0.29	0.24–0.32
9	Islamabad	0.33	0.16–0.24
10	Peshawar	0.33	0.16–0.24
11	Lahore	0.18	0.16–0.24
12	Quetta	0.29	> 0.32
13	Karachi	0.26	0.16–0.24
14	Gwadar	0.29	0.24–0.32

motion values are not uniformly distributed throughout the region; higher hazard is present in the northwestern part. In this study, PGA values for a 475-year RP range from 0.15 to 0.40 g, 0.21 to 0.51 g for 975-year RPs and 0.29 to 0.67 for 2475-year RPs, while SA (0.20 s) and SA (1.0 s) values vary from 0.13 to 0.51 g and 0.64 to 1.59 g, respectively, for the 2475-year RP. The ground motion intensity values (i.e., PGA and SA) in the current study are reported in Table 2 for 19 important cities in Pakistan. Seismic

hazard is highest for the Balakot (PGA 0.36 g), Muzaffarabad (PGA 0.35 g) and Gilgit (PGA 0.34 g) cities corresponding to the 475-year RP.

In order to determine the number of earthquakes with focal depth greater than 50 km (i.e., deep earthquakes) that contribute in the hazard estimation, PSHA is carried out separately using the deep earthquakes. Ground motions are compared to ground motion values obtained by considering all the earthquakes (shallow and deep). A comparison of ground motion values (i.e., PGA values) obtained due to deep and shallow earthquakes has been made for RPs of 475 and 2475 years in Table 3. The distribution of ground motion due to deep earthquakes is shown in Fig. 12.

The BCP (2007) study divided Pakistan into five different seismic zones based on PGA for a 475-year RP: zone 1 from 0.05 to 0.08 g, zone 2A from 0.08 to 0.16 g, zone 2B from 0.16 to 0.24 g, zone 3 from 0.24 to 0.32 g and zone 4 greater than 0.32 g. The upper bound PGA value for zone 4 was not mentioned in BCP (2007). PGA variation in BCP (2007) is 0.08 greater than 0.32 g, whereas the corresponding PGA obtained in this study ranges from 0.15 to 0.40 g. Zone 1 as designated by BCP (2007) does not exist in the seismic hazard map of this study. The upper bound value for zone 4 is also mentioned in the new map (i.e., 0.40 g). It has been also observed that

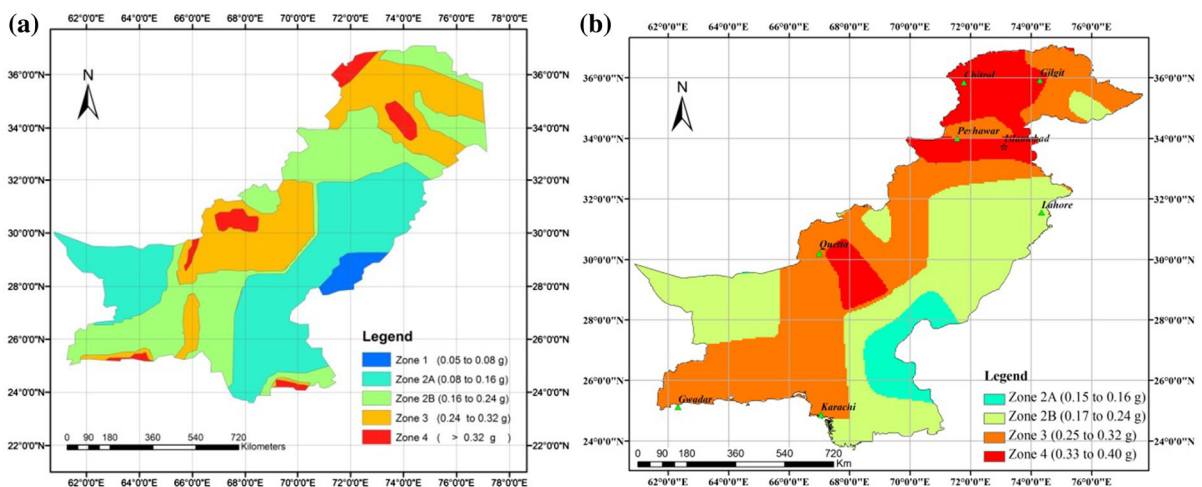


Figure 13  
Comparison of: **a** BCP (2007); **b** current study

the spatial distribution of zones 2–4 has been also changed in the new seismic zoning map. The Peshawar and Islamabad cities which were placed in zone 2B now lie in zone 4. A comparison of the BCP (2007) and the current study is made in Table 4 and Fig. 13.

The comparison of this study with the previous studies is made in terms of PGA only. Zhang et al. (1999) predict PGA in the range of 0.04–0.50 g, while Rafi et al. (2012) suggest this range as 0.004–0.22 g for Pakistan. The seismic hazard maps of Sesetyan et al. (2018b), derived using the Cornell (1968) and Frankel (1995) approaches, recommend a PGA range of 0.02–0.50 g. The PGA range obtained in this study is 0.15–0.40 g. Comparison of the current study with these studies suggests that Sesetyan et al.'s (2018b) results are also in agreement with the current study. Rafi et al.'s (2012) results are on the lower side, and Zhang et al.'s (1999) results are slightly less than this study.

### 5.1. Conclusions

The results of probabilistic seismic hazard assessment suggest an updated seismic hazard map of Pakistan. The following conclusions may be drawn from this study:

1. Higher seismic hazard is present in the regions where the active tectonic features are located, i.e., Makran subduction zone, HinduKush–Pamir and the active fold-and-thrust belt that enters from India and continue in the southwestern direction of Pakistan (includes: Himalaya, Sulaiman and Kirthar mountain ranges).
2. The Sulaiman range in Pakistan has been observed to have the highest seismic hazard in Pakistan (i.e., PGA value of 0.40 g corresponding to a 475-year RP). Among the cities, Balakot, Muzaffarabad, Chitral, Islamabad, Gilgit and Peshawar are the most hazardous.
3. PGA values calculated in this study are higher and are distributed over greater area compared to BCP (2007). The northwestern part placed in zone 2B by BCP (2007) has been changed to zone 4. Therefore, it may be concluded that the BCP (2007) map is under-predicting the ground motion.

The deep earthquakes (i.e., earthquakes having focal depth greater than 70 km) have not been considered by BCP (2007). The higher values obtained are due to the inclusion of deep earthquakes in the analysis and use of recent GMPEs.

4. SA maps for 0.2 and 1.0 s presents ground motion values in line with the recommendations of IBC (2015) and AASHTO-LRFD (2012). These maps are the original contribution for Pakistan, and by using them, earthquake-resistant design may also be carried out in Pakistan based on the recommendations of IBC (2015) and AASHTO-LRFD.
5. Seismic hazard assessment is carried out in this study with the classical approach. Kernel estimation methods of Frankel (1995) and Woo (1996) may also be used for hazard estimation.

### Acknowledgements

The authors acknowledge facilities and the financial support in the purchase of the EZ-FRISK software provided by the National Centre of Excellence in Geology, University of Peshawar, Pakistan, and the EZ-FRISK software, version 7.62, developed for earthquake ground motion prediction. Additionally, the comments and recommendations of the editor and of the anonymous reviewers of the paper are gratefully acknowledged for their constructive review, improving the quality of the article. The various online earthquake data agencies from which data was collected for the earthquake catalogue are acknowledged, including the International Seismological Centre (ISC), National Earthquake Information Center (NEIC), National Geophysical Data Center (NGDC), World Data Centre (WDCse), India Meteorological Department (IMD), Pakistan Meteorological Department (PMD), Micro Seismic Studies Program (MSSP), seismic stations of Mangla and Tarbela dams and the Water and Power Development Authority (WAPDA).

**Publisher's Note** Springer Nature remains neutral with regard to jurisdictional claims in published maps and institutional affiliations.

## REFERENCES

- AASHTO-LRFD. (2012). *Bridge design specifications*. Washington, D.C.: American Association of State Highway and Transportation Officials.
- Ader, et al. (2012). Convergence rate across the Nepal Himalaya and interseismic coupling on the Main Himalayan Thrust: Implications for seismic hazard. *Journal Of Geophysical Research*, 117, 1–16.
- Akkar, S., & Bommer, J. J. (2010). Empirical equation for prediction of PGA, PGV, and spectral acceleration in Europe, the Mediterranean region, and the Middle East. *Seismological Research Letters*, 8(2), 195–206.
- Akkar, S., Sandikkaya, M. A., & Bommer, J. J. (2014). Empirical ground-motion models for point-and extended-source crustal earthquake scenarios in Europe and the Middle East. *Bulletin of Earthquake Engineering*, 12, 359–387.
- Ambraseys, N. (2000). Reappraisal of north-Indian earthquakes at the turn of the 20th century. *Current Science (special edition)*, 79(09), 1237–1250.
- Ambraseys, N., & Bilham, R. (2003). Earthquakes in Afghanistan. *Seismological Research Letters*, 74, 107–123.
- Ambraseys, N., & Bilham, R. (2009). The tectonic setting of Bamiyan and seismicity in and near Afghanistan for the past twelve centuries. In Margottini C (ed) *UNESCO special publication: The destruction of the Giant Buddha statues in Bamiyan, Central Afghanistan, UNESCO's emergency activities for the recovering and rehabilitation of cliff and niches*, vol. 158, pp. 67–94 (ISBN 978-448-0375-5).
- Ambraseys, N., & Douglas, J. J. (2004). Magnitude calibration of north Indian earthquakes. *Geophysical Journal International*, 159, 165–206.
- Apel, E., Burgmann, R., & Nagarajan, B. (2006). Geodetically constrained Indian plate motion and implications for plate boundary deformation. *Eos, Transactions, American Geophysical Union* 85, 52 T51B-1524 Fall meeting supplement.
- Baig, M. S., & Lawrence, R. D. (1987). Precambrian to early Paleozoic orogenesis in the Himalaya. *Kashmir Journal of Geology*, 5, 1–22.
- Bilham, R. (1999). Slip parameters for the Rann of Kachchh, India, 16 June 1819, earthquake, quantified from contemporary accounts. In I. S. Stewart & C. Vita-Finzi (Eds.), *Coastal tectonics* (Vol. 146, pp. 295–318). London: Geological Society.
- Bilham, R., & Ambraseys, N. (2005). Apparent Himalayan slip deficit from the summation of seismic moments for Himalayan earthquakes, 1500–2000. *Current Science*, 88(10), 1658–1663.
- Bilham, R., Lodhi, S., Hough, S., Bukhary, S., Khan, M. A., & Rafeeqi, S. F. A. (2007). Seismic hazard in Karachi, Pakistan: Uncertain past, uncertain future. *Seismological Research Letters*, 78(6), 601–613.
- Bommer, J. J., Douglas, J., Scherbaum, F., Cotton, F., Bungum, H., Faeh, D., et al. (2010). On the selection of ground-motion prediction equations for seismic hazard analysis. *Seismological Research Letters*, 81, 783–793.
- Boore, M. D., Stewart, P. J., Jonathan, P., Seyhan, E., & Gail, M. A. (2014). NGA-West2 equations for predicting PGA, PGV, and 5% damped PSA for shallow crustal earthquakes. *Earthquake Spectra*, 30(3), 1057–1085.
- Building Code of Pakistan: Seismic Provisions (2007) *Ministry of Housing and Society, Government of Pakistan*.
- Cornell, C. A. (1968). Engineering seismic risk analysis. *Bulletin of Seismological Society of America*, 58(05), 1583–1606.
- Cotton, F., Scherbaum, F., Bommer, J. J., & Begum, H. (2006). Criteria for selecting and adjusting ground-motion models for adjusting for specific target regions: Applications to central Europe and rock sites. *Journal of Seismology*, 10, 137.
- Desio, A. (1963). Review of the geologic “formations” of the western Karakorum (central Asia). *Rivista Italiana di Paleontologia e Stratigrafia*, 69, 475–501.
- EZ-FRISK software for earthquake ground motion estimation, version 7.62. Risk Engineering, Inc, USA.
- Frankel, A. (1995). Mapping seismic hazard in the central and eastern United States. *Seismological Research Letters*, 66(4), 8–21.
- Fukushima, Y., & Tanaka, T. (1990). A new attenuation relation for peak horizontal acceleration of strong earthquake ground motion in Japan. *Bulletin of Seismological Society of America*, 80, 757–783.
- Gansser, A. (1981). The geodynamic history of the Himalaya. In H. K. Gupta & F. M. Delany (Eds.), *Zagros, Hindu Kush, Himalaya: Geodynamic evolution* (pp. 111–121). Washington: AGU.
- Gardner, J. K., & Knopoff, L. (1974). Is the sequence of earthquakes in Southern California, with aftershocks removed, Poissonian? *Bulletin of Seismological Society of America*, 64(5), 1363–1367.
- Gulan, L., & EMME WP 2 Team. (2014). *Earthquake Model of the Middle East (EMME) project. Active faults and seismic sources, Second European conference on Earthquake Engineering and Seismology, Istanbul*, August 25–29.
- Gutenberg, B., & Richter, C. F. (1956). Earthquake magnitude, intensity, energy, and acceleration (second paper). *Bulletin of Seismological Society of America*, 46(2), 105–145.
- Heidarzadeh, M., Pirooz, M. D., Zaker, N. H., Yalciner, A. C., Mokhtari, M., & Esmaeili, A. (2008). Historical tsunami in the Makran Subduction Zone off the southern coasts of Iran and Pakistan and results of numerical modeling. *Ocean Engineering*, 35, 774–786.
- IBC. (2015). *International Building Code, International Code Council (ICC), ICC 700*.
- Joyner, W. B., & Boore, D. M. (1981). Peak horizontal acceleration and velocity from strong-motion records including records from the 1979 Imperial Valley, California, earthquake. *Bulletin of Seismological Society of America*, 71(6), 2011–2038.
- Kanno, T., Akria, N., Morikawa, N., Fujiwara, H., & Fukushima, Y. (2006). A new attenuation for strong ground motion in Japan based on recorded data. *Bulletin of Seismological Society of America*, 96(3), 879–897.
- Khan, S., Waseem, M., Khan, M. A., & Ahmed, W. (2018). Updated earthquake catalogue for seismic hazard analysis for Pakistan. *Journal of Seismology*. <https://doi.org/10.1007/s10950-018-9736-y>.
- Kramer, S. L. (1996). *Geotechnical earthquake engineering*. New Jersey: Prentice-Hall.
- Lawrence, R. D., Khan, S. H., & Nakata, T. (1992). Chaman fault, Pakistan–Afghanistan. In R. C. Bucknam, P. L. Hancock (Eds.) *Major active faults of the world—Results of IGCP project 206: Annals Tectonicae*, Supplement to v6, 196–223.
- Martin, S., & Szeliga, W. (2010). A catalog of felt intensity data for 570 earthquakes in India from 1636 to 2009. *Bulletin of Seismological Society of America*, 100, 562–569.

- McGuire, R. K. (1976). *FORTRAN computer program for seismic risk analysis* (pp. 76–6768). Open file Report: United States Geological Survey.
- Mukhopadhyay, B., & Dasgupta, S. (2015). Seismic hazard assessment of Kashmir and Kangra valley region, Western Himalaya, India. *Geomatics, Natural Hazards and Risk*, 6(2), 149–183.
- Mulargia, F., & Tinti, S. (1985). Completeness analysis of a seismic catalogue. *Annals Geophysics*, 3(3), 407–414.
- Nath, S. K., & Thingbaijam, K. K. S. (2012). Probabilistic seismic hazard assessment of India. *Seismological Society of America*, 83(1), 135–149.
- Oldham, T. (1883). A catalogue of Indian earthquakes from the earliest times to the end of 1869 A.D. *Memoirs of the Geological Survey of India*, 19(3), 163–215.
- Quittmeyer, R., & Jacob, K. (1979). Historical and modern seismicity of Pakistan, Afghanistan, northwestern India, and south eastern Iran. *Bulletin of Seismological Society of America*, 69(3), 773–823.
- Rafi, Z., Lindholm, C., Bungum, H., Laghari, A., & Ahmed, N. (2012). Probabilistic seismic hazard map of Pakistan, Azad Jammu and Kashmir. *Natural Hazards*, 61(3), 1317–1354.
- Rahman, M. M., & Bai, L. (2018). Probabilistic seismic hazard assessment of Nepal using multiple source models. *Earth and Planetary Physics*, 2, 327–341.
- Rahman, M. M., Bai, L., Khan, N. G., & Li, G. (2017). Probabilistic seismic hazard assessment of Himalayan–Tibetan region from historical and instrumental earthquake catalogs. *Pure and Applied Geophysics*, 175, 685–705.
- Sawires, R., Pelaez, J. A., Fat-Hebary, R. E. F., & Ibrahim, A. A. (2016). Updated probabilistic seismic hazard values for Egypt. *Bulletin of Seismological Society of America*, 106(04), 1788–1801.
- Sesetyan, K., Demircioglu, B. M., Duman, Y. T., Can, T., Tekin, S., Azak, E. T., et al. (2018a). A probabilistic seismic hazard assessment of the Turkish territory—part I: the area source model. *Bulletin of Earthquake Engineering*, 16(1), 3367–3397.
- Sesetyan, et al. (2018b). The 2014 seismic hazard model of Middle East: Overview and results. *Bulletin of Earthquake Engineering*, 16(08), 3535–3566.
- Shah, M. A., Iqbal, T., Qaiser, M., Ahmed, N., & Tufail, M. (2012). Development of attenuation relationship for northern Pakistan. In *The 15th world conference on earthquake engineering*, Lisbon, Portugal.
- Shedlock, K. M., Giardini, D., Grunthal, G., & Zhang, P. (2000). The GSHAP global seismic hazard map. *Seismological Research Letters*, 71(6), 679–686.
- Stapp, J. C. (1973). Analysis of completeness of earthquake sample in the Punget Sound area in seismic zoning. In Harding, S. T. (Ed.) NOAA Technical Report ERL 267-ESL 30, Boulder, Colorado.
- Stevens, V. L., & Avouac, J. P. (2015). Interseismic coupling on the main Himalayan thrust. *Geophysical Research Letters*, 20, 5828–5837.
- Styron, R., Taylor, M., & Okoronkwo, K. (2010). HimaTibetMap-1.0: New ‘web-2.0’ online database of active structures from the Indo-Asian collision. *Eos*, 91, 20. <https://github.com/HimaTibetMap/HimaTibetMap>.
- Taylor, M., & Yin, A. (2009). Active structures of the Himalayan–Tibetan orogen and their relationships to earthquake distribution, contemporary strain field, and Cenozoic volcanism. *Geosphere*, 05(03), 199–214. <https://github.com/HimaTibetMap/HimaTibetMap>.
- Uniform Building Code (UBC). (1997). *ICBO international conference of building officials, structural engineering design provisions* (Vol. 2). Whittier: Uniform Building Code.
- Waseem, M., Khan, M. A., & Sarfraz, K. (2019). Seismic sources for Pakistan and seismic hazard analysis of Karachi. *Natural Hazards*, 99(1), 511–536.
- Waseem, M., Lai, G. C., & Spacone, E. (2018a). Seismic hazard assessment of northern Pakistan. *Natural Hazards*, 90(2), 563–600.
- Waseem, M., Lateef, A., Ahmad, I., et al. (2018b). Seismic hazard assessment of Afghanistan. *Journal of Seismology*. <https://doi.org/10.1007/s10950-018-9802-5>.
- Wells, D. L., & Coppersmith, K. J. (1994). New empirical relationships among magnitude, rupture length, rupture width, rupture area, and surface displacement. *Bulletin of the Seismological Society of America*, 84(4), 974–1002.
- Wiemer, S. (2001). A software package to analyze seismicity: ZMAP. *Seismological Research Letters*, 72, 373–382.
- Woo, G. (1996). Kernel estimation methods for seismic hazard area source modelling. *Bulletin of the Seismological Society of America*, 88, 353–362.
- Youngs, R. R., Chiou, S. J., Silva, W. J., & Humphrey, J. R. (1997). Strong ground motion attenuation relationships for subduction zone earthquakes. *Seismological Research Letters*, 68(1), 58–73.
- Zaman, S., Ornthammarath, T., & Warnitchai, P. (2012). Probabilistic seismic hazard maps for Pakistan. In *The 15th world conference on earthquake engineering*, Lisbon, Portugal.
- Zhang, P., Yang, Z., Gupta, K. H., Bhatia, C. S., & Shedlock, M. K. (1999). Global seismic hazard assessment program (GSHAP) in continental Asia. *Annali di Geofisica*, 42(06), 1167–1190.
- Zhao, X. J., Zhang, et al. (2006). Attenuation relations for strong ground motion in Japan using site classification based on predominant period. *Bulletin of Seismological Society of America*, 3, 898–913.